Spatiotemporal trends of atmospheric Pb over the last century across inland China

Dejun Wan[a,b,c*], Handong Yang[d], Zhangdong Jin[c,e], Bin Xue[f], Lei Song[a,b], Xin Mao[a,b], Jinsong Yang[a,b]

[a] Institute of Hydrogeology and Environmental Geology, Chinese Academy of Geological Sciences, Shijiazhuang 050061, China

[b] Key Laboratory of Quaternary Chronology and Hydrological Environment Evolution, CAGS, Shijiazhuang 050061, China

[c] State Key Laboratory of Loess and Quaternary Geology, Institute of Earth Environment, Chinese Academy of Sciences, Xi'an 710075, China

[d] Environmental Change Research Centre, University College London, London WC1E 6BT, UK

[e] Institute of Global Environmental Change, Xi'an Jiaotong University, Xi'an 710049, China

[f] State Key Laboratory of Lake Science and Environment, Nanjing Institute of Geography and Limnology, Chinese Academy of Sciences, Nanjing, 210008, China

Commented [A1]: Use mainland instead? If this changed, you should change the rest accordingly.

Abstract

Sedimentary records from remote regions contain pollutants derived dominantly from atmospheric input, and thus have the potential to trace past atmospheric pollution history. Based on seventeen sediment records from relatively remote areas of China, atmospheric Pb pollution history during the last century was studied. These records suggest some slight pollution before ~1950 and display synchronous Pb enrichment processes since the 1950s, implying the start of widespread atmospheric Pb pollution in China. This corresponded well with the beginning of socio-economic development after the establishment of the People's Republic of China. However, owing to the Chinese Cultural Revolution, a roughly unchanged atmospheric Pb status was found in the 1960-70s except on the Qinghai-Tibetan Plateau, where atmospheric Pb still increased gradually caused by long-range atmospheric transport of pollutants from southwest Asia. In ~1980-2000, atmospheric Pb experienced the greatest increase, resulting from rapid development of extensive economy after the Reform and Opening-up in 1978. After ~2000, atmospheric Pb generally stopped increasing due to the phasing out of leaded gasoline, but it remained high, with the highest in Southwest China, medium in Northeast China, central North China and the Qinghai-Tibetan Plateau, and the lowest in the southeast Mongolia Plateau and West China. This study reveals spatio-temporal variations of atmospheric Pb in inland China under the influence of recent human activities, providing an important supplement for understanding global Pb pollution in the Anthropocene.

Deleted: only occasionally

Deleted: the

Commented [A2]: See above.

Keywords: historical record; sediment core; heavy metal; lead isotope; atmospheric pollution; Anthropocene

Commented [A3]: Trace metal? You use the trace metals in the text. Keep the same.

1. Introduction

Lead is a toxic trace metal which has serious adverse effects on human health: Pb poisoning can harm the central and peripheral nervous systems, kidneys, and blood circulation in humans (Cheng and Hu, 2010). Among the trace metals, lead (Pb) is one of the most pervasive and toxic (Marx et al., 2016). Rauch and Pacyna (2009) suggest that the current anthropogenic emissions of Pb are more than 150% of natural emissions, whereas industrial emissions of Cu, Ni and Zn are only 48%, 48%, and 33% of natural emissions, respectively. The three main anthropogenic Pb sources in modern times are leaded gasoline, nonferrous metal production, and fossil fuel combustion (Marx et al., 2016; Rauch and Pacyna, 2009).

In recent decades, Pb pollution history across the globe was widely investigated by analyzing various kinds of natural archives like peat bogs, ice cores, and lake sediments. These investigations suggested that the early presence of human-induced Pb in the environment can be dated back to the mid-Holocene in Europe (García-Alix et al., 2013; Marx et al., 2016; Weiss et al., 1999), North America (Pompeani et al., 2013) and East Asia (Lee et al., 2008). However, the anthropogenic Pb pollution usually occurred in limited sites and in relatively short periods before the Industrial Revolution (Beaudon et al., 2017; Marx et al., 2016; McConnell et al., 2018; Pompeani et al., 2013). The globally ubiquitous pollution of Pb started in the late Nineteenth Century (the Second Industrial Revolution), since then the magnitude of Pb pollution increased dramatically (Marx et al., 2016; Pérez-Rodríguez et al., 2018). However, the toxicity of the lead in the environment was not widely recognized until the 1950s-1960s and in the following

Deleted: over

Deleted: sedimentary record

Deleted: lead

Deleted: after

decades it has attracted great concern from environmentalists (Marx et al., 2016). Since the 1970-1980s, anthropogenic Pb emissions in developed countries have been reduced considerably because of industrial emission controls and the phasing out of leaded gasoline (Marx et al., 2016). For example, it is estimated that atmospheric Pb emissions in 1970 were ~220000 and ~82000 tons in the USA and Western and Central Europe, respectively, whereas emissions in 2000 were only ~3000 and ~4000 tons, respectively (Marx et al., 2016). On the whole, Pb emissions in these countries have been effectively controlled in recent decades.

Compared to developed countries, the increase of modern anthropogenic Pb in China started later (mostly post-1950s) and accelerated since the 1970s-1980s owing to the rapid development of society and economy after the Reform and Opening-up in 1978. Tian et al. (2015) estimated that atmospheric Pb emissions in China were only ~3800 tons in 1970 but increased to ~20000 tons in 2000. Although leaded gasoline was phased out in 2000 AD and atmospheric Pb emissions decreased by approximately two-thirds in 2001, in the following years the emissions quickly increased again (Li et al., 2012; Tian et al., 2015). In 2012, Pb emissions again reached ~14000 tons (Tian et al., 2015). In the last decade, Pb pollution incidents in China occurred more frequently than before. For instance, in 2004-2012, more than 50 cases of group (more than 19 people) blood lead excess caused by Pb pollution were reported (Lv et al., 2013).

Long-term pollution history is important in understanding the influence of recent human activities on the environment and pollution control. In recent years, a few investigations have evaluated Pb pollution history in recent centuries based on various

Deleted: the

kinds of natural archives such as lake sediment cores, peat and ice cores from both relatively remote areas (e.g. Bao et al., 2016; Beaudon et al., 2017; Li et al., 2017; Zhang et al., 2014) and populated areas (e.g. Li et al., 2018; Yao and Xue, 2014; Yu et al., 2016; Zhang et al., 2016) in China. According to sedimentary records from China covering the last millennia, it was suggested that anthropogenic Pb pollution occurred hundreds or even thousands years ago related to mining and metallurgy, such as in Lake Liangzhi since ~3000±328 BC in central China (Lee et al., 2008) and in Lake Erhai from 1100 to 1300 AD in southwest China (Hillman et al., 2015). However, these pollutions were usually related to local human activities and had little relation with regional atmospheric pollution in remote China.

Deleted: the

Deleted: the

Deleted: release

Although few human industrial activities occur in relatively remote areas of China, investigations in these areas such as Lake Qinghai (Jin et al., 2010), Lake Ngoring (Zhang et al., 2014), Puruogangri (ice core) (Beaudon et al., 2017), Lake Fuxian (Liu et al., 2013), and Lake Sayram (SR) (Zeng et al., 2014) found increases of anthropogenic Pb in recent several decades. The reconstructed anthropogenic Pb fluxes in the 21st century vary greatly (from several to dozens mg m^{-2} yr^{-1}) among these records (Jin et al., 2010; Liu et al., 2013; Zeng et al., 2014; Zhang et al., 2014). Owing to anthropogenic Pb in these remote areas derived dominantly from regional atmospheric deposition, the above changes indicate increases of atmospheric Pb, but with different levels of increase over China. These studies provide valuable data for understanding atmospheric Pb pollution in remote areas of China in the past. However, as most of these studies are individual cases, they usually only have local implications

and do not give a comprehensive study of Pb pollution history in China. Hence, it is necessary to investigate reliable sediment records from different regions of China to comprehensively understand the temporal patterns of past Pb pollution.

In this study, an investigation of anthropogenic Pb history during the last one or two centuries was carried out based on enrichment factors (EFs), reconstructed anthropogenic fluxes, and Pb isotopes in seventeen sediment records from relatively remote areas of China. Given that anthropogenic Pb in these records was mainly derived from atmospheric input (Bao et al. 2015, 2016; Beaudon et al., 2017; Li et al., 2017; Liu et al., 2013), they likely reflect past atmospheric Pb pollution in China. Therefore, the main objectives of this work are to reveal temporal and spatial variations of atmospheric Pb in the last century in relatively remote areas of China and to discuss influence factors of atmospheric Pb evolution, especially the relation with socioeconomic development. This study is helpful in understanding the influence of recent human activities on atmospheric pollution and in formulating policies to mitigate trace metal pollution in China. In addition, given China's considerably large Pb emissions and its specific evolution pattern, this study is an important supplement to understanding Pb pollution on a global scale.

Deleted: heavy

Deleted: mparative

2. Materials and methods

2.1. Study area and sediment core sampling

Since East China is densely populated and most lakes are disturbed by direct human activities, six lakes, Gonghai (GH), Maying (MY), Dali (DL), Zhagesitai (ZGST),

Wudalianchi-3 (WDLC-3), and Wudalianchi-5 (WDLC-5) (Fig. 1), in inland areas of China were selected for sampling. These lakes are all located in relatively remote areas (with negligible industrial emissions compared with urban areas). The geological setting of these lakes and details of the sediment cores are shown in SM Text S1 and Table S1.

One sediment core was recovered from each lake using a gravity corer between 2009 and 2016. All cores were retrieved in lake centers or deep-water areas. More details of core sampling are given in Table S1. The sediment cores were sliced at 1-cm intervals. After dried at either < -20 °C under vacuum with a freeze dryer or at 40-60 °C in an oven, the sediment samples were packed in plastic bags and stored in desiccators. Subsamples of the sediments were ground to powder with particles < 63 μm for chemical analysis.

In addition, we obtained the Pb records published in recent years in China, from relatively remote areas for comparison. Eleven sediment records from reported studies were compiled (Fig. 1). Most of them are lake sediments (Jin et al., 2010; Liu et al., 2013; Zeng et al., 2014; Zhang et al., 2014a,b; Bing et al., 2016; Li et al., 2017), but two peat cores (Bao et al. 2015, 2016) and one ice core (Beaudon et al., 2017) were also included. Lead concentrations in these compiled sediment records were obtained with ICP-MS or ICP-AES similar to our analyses, so the compiled Pb data can be compared with those in our records.

Commented [A4]: Northeast China?

Deleted: ection**e**

Deleted: , for comparison,

Deleted: correspond to

Deleted: an

Deleted: The Pb

Deleted: ary

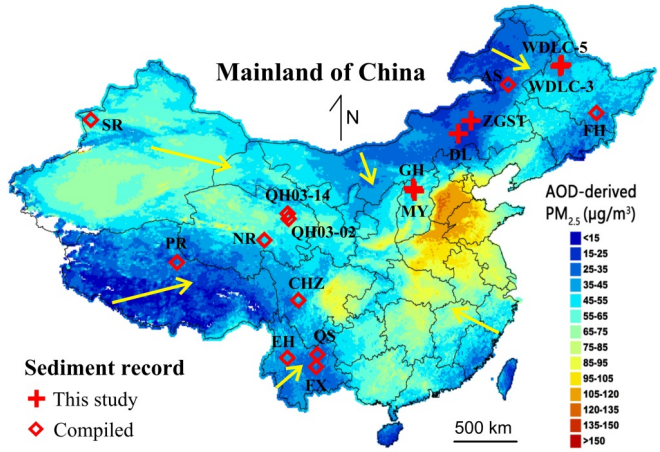

167

168 **Fig. 1** (**a**) Sediment cores retrieved from lakes of Wudalianchi-3 (WDLC-3),

169 Wudalianchi-5 (WDLC-5), Zhagesitai (ZGST), Dali (DL), Gonghai (GH), and Maying

170 (MY). Also shown are eleven compiled records from reported studies from lakes of

171 Sayram (SR) (Zeng et al., 2014), Ngoring (NR) (Zhang et al., 2014) , Qinghai (QH) (Jin

172 et al., 2010), Caohaizi (CHZ) (Bing et al., 2016), Erhai (EH) (Li et al., 2017), Qingshui

173 (QS) and Fuxian (FX) (Liu et al., 2013), and Puruogangri (PR, ice core) (Beaudon et

174 al., 2017), Aershan (AS, peat cores) (Bao et al., 2015), and Fenghuang (FH, peat cores)

175 (Bao et al., 2016). Colors represent spatial distributions of the 10-year (2004-2013)

176 mean AOD (satellite-retrieved aerosol optical depth)-derived $PM_{2.5}$ levels over China

177 (Ma et al., 2016). Arrows represent major atmospheric circulation directions in China

178 (Chen et al., 1991).

Deleted: the

179 **2.2. Enrichment factors (EFs)**

180 EFs are among the most commonly used indexes to assess trace metal pollution in

181 environmental media and to evaluate natural and anthropogenic sources. The EF of Pb

in a sediment sample can be calculated using the following equation (Liu et al., 2013; Wan et al., 2016a):

$$EF = (Pb / Ti)_s / (Pb / Ti)_b \quad (1)$$

where s and b represent sediment samples and backgrounds, respectively. Titanium (Ti), which is a conservative lithogenic element and shows relatively minor variations in these cores, was selected as the reference element like many other studies (Bao et al., 2015; Jin et al., 2010; Li et al., 2017; Liu et al., 2013). The background of Pb or Ti in a sediment core is the average of Pb or Ti concentrations in the bottom core sections (Fig. S1), where the sediments that have not been contaminated by Pb and have low and stable Pb concentrations and high and stable $^{206}Pb/^{207}Pb$ ratios. In detail, the background values were averages of Pb or Ti concentrations in the bottom cores sections of GH (30-60 cm, 1786-1913), MY (30-56 cm, 1784-1916), DL (26-30 cm, 1902-1920), ZGST (36-40 cm), WDLC-3 (36-49 cm, 1926-1949), and WDLC-5 (31-40 cm, 1936-1949).

Deleted: core

2.3. Lead fluxes

Anthropogenic Pb fluxes ($Pb[Flux_{anthropogenic}]$, mg m^{-2} yr^{-1}) were calculated according to the following equations by using Ti as the reference element (Jin et al., 2010; Wan et al., 2019):

$$Pb[Flux_{anthropogenic}] = (Pb[C_{sample}] - Pb[C_{background}] \times Ti[C_{sample}]/Ti[C_{background}]) \times R \times \rho \quad (2)$$

where $Pb[C_{sample}]$ and $Pb[C_{background}]$ represent sample and background concentrations of Pb in sediments, respectively, R is the sedimentation rate (cm yr^{-1}), and ρ is the dry bulk density (g cm^{-3}) of the sediments. $Ti[C_{sample}]$ and $Ti[C_{background}]$ represent the sample and background concentrations of Ti in the sediments, respectively.

Negative values which represented no anthropogenic Pb contributions and were caused by that averages of Pb concentrations in the bottom sections employed as the background and that there were some slight natural variations of Pb or Ti in these sections. These negative values were all set to zero in the cores.

Other information for sample analyses can be found in SM Text S2.

3. Results

3.1 Sediment core dating

As ^{210}Pb occurs naturally as one of the radionuclides in the ^{238}U decay series and anthropogenic Pb consists of ^{204}Pb, ^{206}Pb, ^{207}Pb, and ^{208}Pb but not ^{210}Pb (Appleby, 2001), it can be used to assess the chronology of polluted sediment cores with Pb from anthropogenic sources. Generally, $^{210}Pb_{ex}$ activities in cores of GH and DL decrease more or less following an exponential trend with depth and reach equilibrium with total ^{210}Pb activities at their bottom sections (Fig. S2). The two sediment cores were dated by using the constant rate of ^{210}Pb supply (CRS) model (Appleby, 2001). Additionally, ^{137}Cs peaks (such as the 1963 peak) in these cores were also employed to further restrict the CRS dating results (Anjum et al., 2017; Lan et al., 2018). Due to the relatively large uncertainties of the CRS ages at the bottom sections of GH (30-60 cm) and DL (25-30 cm) cores, possibly caused by low $^{210}Pb_{ex}$ activities with relatively high counting errors, we have extrapolated ages for these sections by using the average sedimentation rate in the middle (10-20 cm) core section. Considering that these extrapolated ages were all pre-1930 and Pb pollution occurred mainly after ~1950 (Fig. 2), such estimations

Deleted: were

Deleted: se

Deleted: herefore, t

Deleted: the

Deleted: in

Deleted: but unstable

should have little influence on the main conclusions in this study. More dating details can be found in our previous works of Wan et al. (2019a; 2019b) for these two cores. Considering similar Pb profiles in the ZGST and DL cores and the short distance (~50 km) between the two lakes, the ZGST core was not dated and only used for comparison with the DL core.

In the MY core, ^{137}Cs activity shows similar variation trend to that of GH (Fig. S2). It has a clear peak at 19-cm depth which can be considered as a time marker for 1963. Although the $^{210}Pb_{ex}$ activities in MY are also similar to those in GH, their variation trend for MY is abnormal. The $^{210}Pb_{ex}$ activities increase from 201 Bq kg^{-1} in the top 0-1 sediment to 248 Bq kg^{-1} in the 4-5 cm sediment and shows no exponential decreasing trend in the top 9 cm core section. The core was also dated with the CRS model. However, the model yielded ages are very different from those suggested by the 1963 ^{137}Cs peak, which may be due to the abnormal variation trend of $^{210}Pb_{ex}$ activities in the 0-9 cm section of the core. Hence, the MY core was dated by using an average mass sedimentation rate (0.2145 g cm^{-2} yr^{-1}) calculated based on the clear 1963 ^{137}Cs peak at 19-cm depth (Fig. S2). Considering that the lake has a similar geological setting to that of GH that has a relatively stable sedimentation rate, it is reasonable to extrapolate ages by using the average sediment rate obtained by ^{137}Cs. Moreover, comparing Pb profiles between the MY and GH cores shows synchronous variations (Fig. 2), implying acceptable errors of the estimated ages for the MY core.

The chronologies of the WDLC-3 and WDLC-5 cores were after that in Gui et al. (2012). Briefly, in WDLC-3 and WDLC-5, the ^{137}Cs activities were first detected at 34

cm and 32 cm and reached their first peak at 27 cm and 21 cm, respectively (Fig. S2). The peaks of ^{137}Cs for both cores were clear, and thus they can be considered as a time marker for 1963. The $^{210}Pb_{ex}$ activities in the top sediments of the two cores are similar and comparable to the median of that in eleven lakes in this province (Pratte et al., 2019). Compared to GH, MY and DL, the $^{210}Pb_{ex}$ activities in WDLC top sediments are higher, reflecting regional differences of the atmospheric $^{210}Pb_{ex}$ deposition. As $^{210}Pb_{ex}$ activities did not reach equilibrium with ^{226}Ra in both cores, it was not suitable to estimate the sediment ages by using the ^{210}Pb CRS model. Based on the ^{210}Pb CIC model, age of the mid-1920s was obtained at the 27 cm depth in WDLC-3. This result differed significantly from that inferred from the ^{137}Cs peak, implying great uncertainties of this dating result that was caused by abnormal $^{210}Pb_{ex}$ values in the 20-30 cm section of the core likely related to reclamation around the lake area. Hence, using the first peak of ^{137}Cs activity in 1963 as a time marker, the composite model of ^{210}Pb (Appleby, 2001) was employed to determine sediment ages of WDLC-3. Similarly, the composite model was also used to date sediment ages in WDLC-5 post the early 1960s. Assuming uniform sediment rates in the bottom cores sections (before the early 1960s), ages in the core bottoms were calculated to be 1926 in WDLC-3 and 1936 in WDLC-5. The average mass sediment rates were 0.28 g cm^{-2} yr^{-1} (0.59 cm yr^{-1}) in WDLC-3 and 0.25 g cm^{-2} yr^{-1} (0.55 cm yr^{-1}) in WDLC-5. The WDLC-3 core covered a period of 1926-2009 and the WDLC-5 of 1936-2009.

The time resolutions in the post-1900 and the post-1950 sediments are 3.5 and 2.8 yr cm^{-1} in GH, 3.4 and 2.9 yr cm^{-1} in MY, 3.8 and 3.1 yr cm^{-1} in DL, 1.7 and 1.7 yr cm^{-}

Deleted: come into

$^{-1}$ in WDLC-3, and 1.8 and 2.0 yr cm^{-1} in WDLC-5, respectively. The top core sections usually have relatively higher time resolutions as they contain more water. It should be noted that when sampling use a gravity corer, the top several-centimeters of the core may be disturbed. This may lead to dating uncertainties, but the uncertainties were likely minor considering relatively high sediment rates in the top 3-cm sections of these sediment cores which were 1.0 cm yr^{-1} for GH, 0.67 cm yr^{-1} for MY, 0.58 cm yr^{-1} for DL, 0.57 cm yr^{-1} for WDLC-3 and 1.0 cm yr^{-1} for WDLC-5.

3.2. Lead concentrations

Lead concentrations in the cores of GH, MY, DL, ZGST, WDLC-3, and WDLC-5 have ranges of 18.5-24.8, 19.6-25.7, 16.6-20.1, 12.7-18.5, 29.8-34.8, and 29.5-37.1 mg kg^{-1} and averages of 21.2±2.0, 22.7±2.5, 18.4±1.2, 15.6±1.6, 32.0±1.3, and 33.3±1.7 mg kg^{-1}, respectively. Considering that elemental background concentrations, depending on the catchment lithology and soils, may strongly differ between lakes, the background Pb values in the lakes of GH, MY, DL, ZGST, WDLC-3, WDLC-5 were calculated by averaging the Pb concentrations in their bottom core sections where there is little anthropogenic pollution.

In these records, variations of their Pb concentrations are modest (12.7 to 37.1 mg kg^{-1}) (Fig. 2 and Fig. S3). The lowest Pb concentrations are found in the ZGST core, with an average of 15.6 mg kg^{-1} and a maximum of 18.5 mg kg^{-1}; the highest concentrations are found in the WDLC-5 core, with a maximum of 37.1 mg kg^{-1}. However, the differences are mainly related to different natural Pb background values

Deleted: ,

Deleted: ithout

in these lakes rather than pollution. For example, the average Pb concentration is only 12.7 mg kg^{-1} in the background sediments (bottom section) of the ZGST core, while that in the WDLC-5 core is 29.5 mg kg^{-1}. Compared with other lake sediment records from relatively remote areas of China (Fig. 2), our Pb results are close to those in NR (Zhang et al., 2014), QH03-2 and QH03-14 (Jin et al., 2010) from the Qinghai-Tibetan Plateau and SR from West China (Zeng et al., 2014) (Fig. 1), but they are remarkably lower than those in southwest China (FX and QS, Liu et al., 2013; EH, Li et al., 2017) (Fig. 1), which is also caused by high (~60 mg kg^{-1}) Pb background values in these lakes in southwest China.

Deleted: and

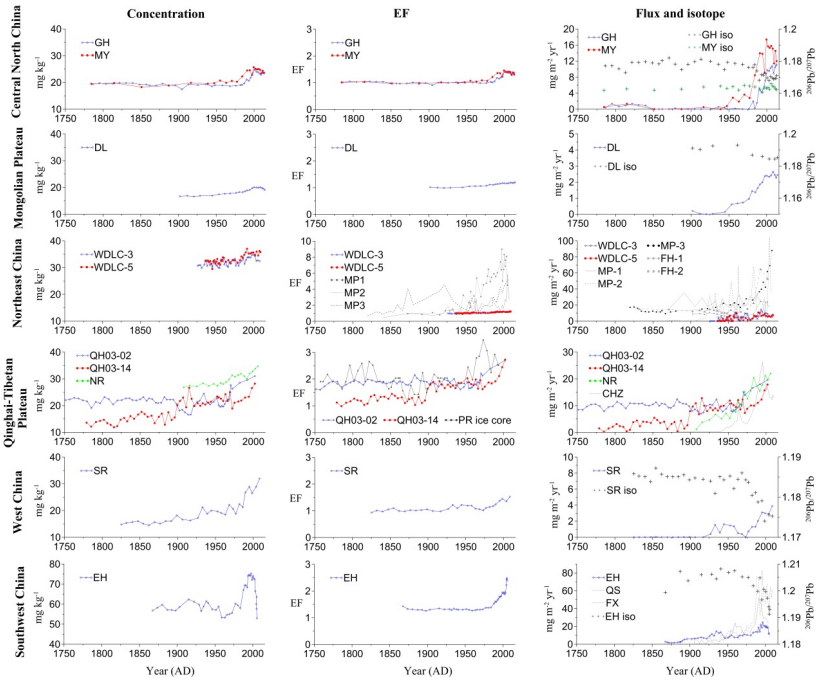

Fig. 2 Pb concentrations, EFs, anthropogenic fluxes, and isotopes in lake sediment cores of GH, MY, DL, WDLC-3, WDLC-5 (Table S3), QH03-02 and QH03-14 (Jin et al.,

2010), NR (Zhang et al., 2014), CHZ (Bing et al., 2016), SR (Zeng et al., 2014), EH (Li et al., 2017), FX and QS (Liu et al., 2013), and peat cores of MP and FH (Bao et al., 2015 and 2016), and an ice core of PR (5-year average, Beaudon et al., 2017) in China.

3.3 Pollution indices——Pb EFs, anthropogenic fluxes and isotopes

Considering bulk Pb concentrations may not reflect past pollution variations in sediment records as they are often affected by sedimentation processes such as changes in sediment accumulation rate and contents of organic matter and carbonate, EFs and anthropogenic fluxes were calculated and Pb isotopes were analyzed to understand anthropogenic pollution in these cores (Fig. 2). The Pb EFs in the cores of GH, MY, DL, ZGST, WDLC-3, and WDLC-5 have ranges of 0.91-1.41, 0.97-1.46, 0.98-1.20, 0.93-1.31, 0.94-1.21, and 0.93-1.23 and averages of 1.10±0.16, 1.19±0.18, 1.10±0.07, 1.14±0.10, 1.06±0.07, and 1.08±0.08, respectively. The anthropogenic Pb fluxes in the cores of GH, MY, DL, WDLC-3, and WDLC-5 have ranges of 0-11.2, 0-17.4, 0-2.6, 0-14.5, and 0-10.7 mg m^{-2} yr^{-1} and averages of 3.0±4.1, 7.7±6.6, 1.4±1.0, 4.6±3.9, and 4.3±3.3 mg m^{-2} yr^{-1}, respectively. The $^{206}Pb/^{207}Pb$ ratios in the cores of GH, MY, DL, and ZGST have ranges of 1.1679-1.1820, 1.1606-1.1659, 1.1843-1.1929, and 1.1740-1.1902 and averages of 1.1753±0.0042, 1.1632±0.0012, 1.1882±0.0035, and 1.1826±0.0048, respectively.

From their profiles in Fig. 2, it can be seen that both the Pb EFs and anthropogenic fluxes in these cores show obvious increases in recent several decades, whereas the $^{206}Pb/^{207}Pb$ ratios decrease synchronously except MY. Besides our records, the

Deleted: ry

Deleted: further

$^{206}Pb/^{207}Pb$ ratios from other records in relatively remote areas of China, e.g. Lake Sayram (SR) (Zeng et al., 2014), Aershan (AS, peat cores) (Bao et al., 2015), Lake Fuxian (FX) (Liu et al., 2013), Lake Qingshui (QS) (Liu et al., 2013), and Lake Erhai (EH) (Li et al., 2017), also show similar decreases in recent decades. The widespread and obvious decreases of $^{206}Pb/^{207}Pb$ ratios in recent decades in these records imply possible changes in Pb sources. A comparison of various Pb sources in China (Fig. 3) suggests that the $^{206}Pb/^{207}Pb$ and $^{208}Pb/^{207}Pb$ ratios in sediments pre-1980 were close to those of natural sources such as loess and desert dust samples in North China (Ferrat et al., 2012), whereas the $^{206}Pb/^{207}Pb$ and $^{208}Pb/^{207}Pb$ ratios in recent sediments (post-1980) were deviating from those of the natural sources but close to anthropogenic sources, such as urban aerosols (Chen et al., 2005; Mukai et al., 2001; Wang et al., 2006) and Chinese Pb ore and coal (Cheng and Hu, 2010). However, as anthropogenic Pb in these records derived mainly from heavily mixed sources via regional atmospheric transport and few Pb isotope data available in these remote lake areas, detailed point sources of the anthropogenic Pb were likely unable to be identified.

The changes above are similar to many other Pb isotope studies in China, those suggest that the changes were mainly related to anthropogenic Pb inputs (Liu et al., 2013; Yu et al., 2016; Zhang, et al., 2016). In combination with the synchronous increases in EFs and anthropogenic fluxes, it is reasonable to infer that the above Pb isotope changes were caused by increased inputs of anthropogenic Pb in recent decades. Although it is not the most ideal approach to determine Pb isotope by using an ICP-MS, the accuracy is high enough to differentiate Pb isotopes in natural sediments from

Deleted: like

Deleted: getting

Deleted: above

Deleted: s

Deleted: which

Deleted: ed

Deleted: as

Deleted: ing

anthropogenic sources as indicated by their coherent changes in these records except MY. The lack of a decrease in $^{206}Pb/^{207}Pb$ in MY could not be caused by that this Pb record was already contaminated by anthropogenic sources before the Eighteenth Century as another lake (GH), only 5 km away from MY, showed no anthropogenic Pb signals until 1970s (Fig. 2). It was probably due to the fact that background Pb isotopic ratios in its non-polluted sediment are similar to those of the anthropogenic sources such as urban aerosols (Fig. 3). Even during 1980-2014 the $^{206}Pb/^{207}Pb$ ratios in MY remained approximate 1.164±0.002 that were almost similar to those (about 1.1625) before 1900. Another lake

Commented [A5]: Delete it? Pay attention to this!

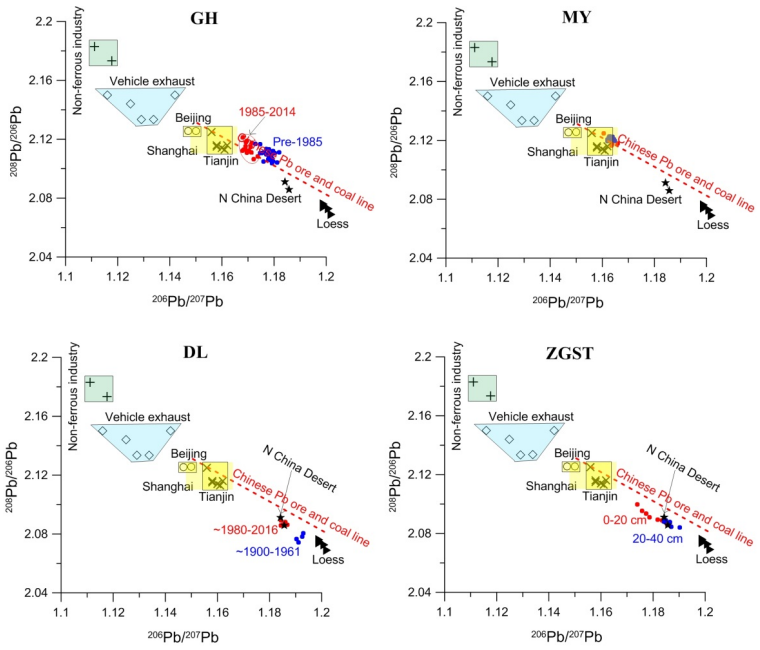

Fig. 3 A comparison of Pb isotopes in sediment cores of GH, MY, DL, and ZGST (red and blue solid dots) (Table S4) with those in Chinese Pb ore and coal (Cheng and Hu, 2010), vehicle exhaust (Liu et al., 2004; Wang et al., 2002; Zheng et al., 2004),

nonferrous industrial materials (Liu et al., 2004; Wang et al., 2002; Zheng et al., 2004), urban aerosols from Beijing (Mukai et al., 2001), Tianjin (Wang et al., 2006) and Shanghai (Chen et al., 2005), and N. China deserts (Tengger and Badain Jaran) and loess (Loess Plateau) (Ferrat et al., 2012).

4. Discussion

4.1. Implication of anthropogenic Pb pollution

Lead from anthropogenic emission sources in lake sediments is mainly derived from three pathways: direct dumping, catchment erosion, and atmospheric wet and dry deposition (Chen et al., 2016; Wan et al., 2019b). As these lakes are all located in relatively remote areas of China, there are few local pollution sources around the lakes and within their catchments, so direct additions of anthropogenic Pb are negligible. Second, catchment erosion brings naturally occurring Pb into the lake, at the same time it may also bring a certain amount of anthropogenic Pb that was transported to the lake catchment through atmospheric deposition. These facts suggest that the anthropogenic Pb in these lake sediments is dominantly derived from atmospheric Pb transport and deposition. Hence Pb pollution signals in these records have the potential to reflect past regional atmospheric Pb pollution.

Deleted: se

Deleted: the

4.2. Temporal variations of atmospheric Pb pollution in China

To reveal the spatio-temporal variations of atmospheric Pb pollution in China, representative Pb records in relatively remote areas of China from reported studies

were compiled. However, considering large differences in the reconstructed Pb fluxes of peat records even from the same area (AS and FH, Bao et al., 2015 and 2016), the fluxes were not included for calculating average fluxes in Fig. 4. They are only employed for comparing evolution trends of atmospheric Pb in recent centuries. Besides, owing to large uncertainties in anthropogenic Pb fluxes in QH, recalibrated fluxes were used in Fig. 4 (discussed in the following paragraph). Based on temporal variations of Pb fluxes and other pollution indices of EFs and Pb isotopes in the six regions of China (Fig. 2 and 4), four evolution stages of atmospheric Pb during the last century were divided.

Deleted: when

Deleted: o

Deleted: the

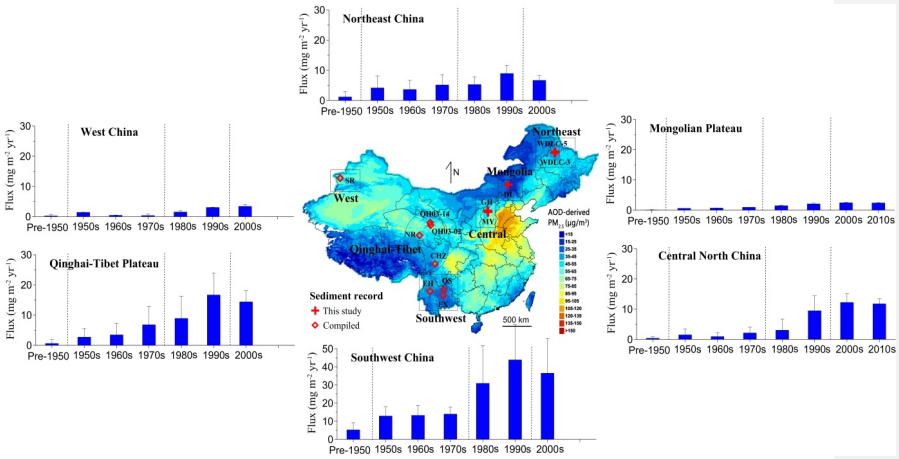

Fig. 4 Average anthropogenic Pb fluxes (Table S5) in different periods from Northeast China (WDLC-3 and WDLC-5), West China (SR (Zeng et al., 2014)), the Mongolian Plateau (DL), the Qinghai-Tibet Plateau (NR (Zhang et al., 2014), CHZ (Bing et al., 2016) and QH (recalibrated, Jin et al., 2010), Central North China (GH and MY), and Southwest China (EH (Li et al., 2017), QS and FX Liu et al., 2013).

Before ~1950, atmospheric Pb in these relatively areas of China experienced negligible anthropogenic Pb pollution except some slight pollution events. The average anthropogenic Pb fluxes before ~1950 were the lowest and close to zero in the six regions of China except Southwest China (Fig. 4). The detailed Pb variations in Fig. 2 show that the fluxes as well as EFs were relatively stable except some occasionally slight increases in GH and MY during the 1780s-1840s, in MP-1 during the 1890s and 1910s, in MP-2 during the 1920s-1930s, in PR during the 1800s-1820s, in SR during the 1930s-1940s, and in EH during 1890-1940. First, the high flux (5.2±4.0 mg m^{-2} yr^{-1}) before 1950 in Southwest China (Fig. 4) was mainly caused by increases in 1890-1940 in EH (Li et al., 2017) (Fig. 2). However, it is suggested that the increase in EH in 1890-1940 had no relation with anthropogenic Pb pollution by analyzing Pb isotopes and EFs (Li et al., 2017), which was also supported by FX and QS records from the same region (Liu et al., 2013). This implies negligible atmospheric Pb pollution in Southwest China in 1900-1950. Second, the QH03-14 shows an obvious increase from 2.7 mg m^{-2} yr^{-1} before ~1900 to 9.2 mg m^{-2} yr^{-1} in ~1900 (Jin et al., 2010) (Fig. 2). In contrast, another core of QH03-02 from the same lake shows an obvious decrease in Pb concentration synchronously (Fig. 2). Hence, it can be inferred that the increase in QH03-14 fluxes were likely resulted from natural causes likely to be source changes rather than anthropogenic pollution. Considering the large uncertainties in anthropogenic Pb fluxes in QH, the fluxes in these two cores were recalibrated for Fig. 4 by subtracting average fluxes during ~1750-~1950 in QH03-02 (9.8 mg m^{-2} yr^{-1}) and during ~1900-~1950 in QH03-14 (9.3 mg m^{-2} yr^{-1}), respectively. Third, another

Deleted: the

Deleted: occasionally

Deleted: o

Deleted: before calculating values in

exception was the peat cores. Although the fluxes in most of the peat cores were also generally stable before ~1950, their values were as high as ~10 mg m^{-2} yr^{-1}. Considering these two sites are relatively remote, we can infer that the long-lasting stable high fluxes before ~1950 were related to reconstruction uncertainties than anthropogenic pollution. Fourth, the Pb EFs in most samples in the PR ice core were ~2 before ~1950 and even before 1750 AD (Beaudon et al. 2017). The high values in the core were not related to pollution but likely caused by the Tibetan Plateau aeolian dust.

The negligible atmospheric Pb pollution before 1950 was in accordance with the extremely lacking status of socioeconomic development in China. Before 1949, the People's Republic of China was not founded and China was engaged in war for decades, its economy and industry were poor and dominated by a small quantity of light industries such as textile and flour mainly distributed in some coastal cities like Shanghai, Tianjin, and Guangzhou (WGEDHC, 2016). Similarly, the estimated atmospheric Pb emissions (Tian et al., 2015) also show a negligible Pb emission in China in 1949 (Fig. 5). However, the atmosphere in China may be affected by extremely low level anthropogenic Pb transported by global atmospheric circulation from sources in developed countries after the Industrial Revolution. However, concentrations were too low to be detected by the above records.

Commented [A6]: Natural peat focusing process(?)

Deleted: more

Deleted: dust samples from Potential Source Areas of

Deleted: as background materials to calculate EF

Deleted: before ~1950

Deleted: lacking

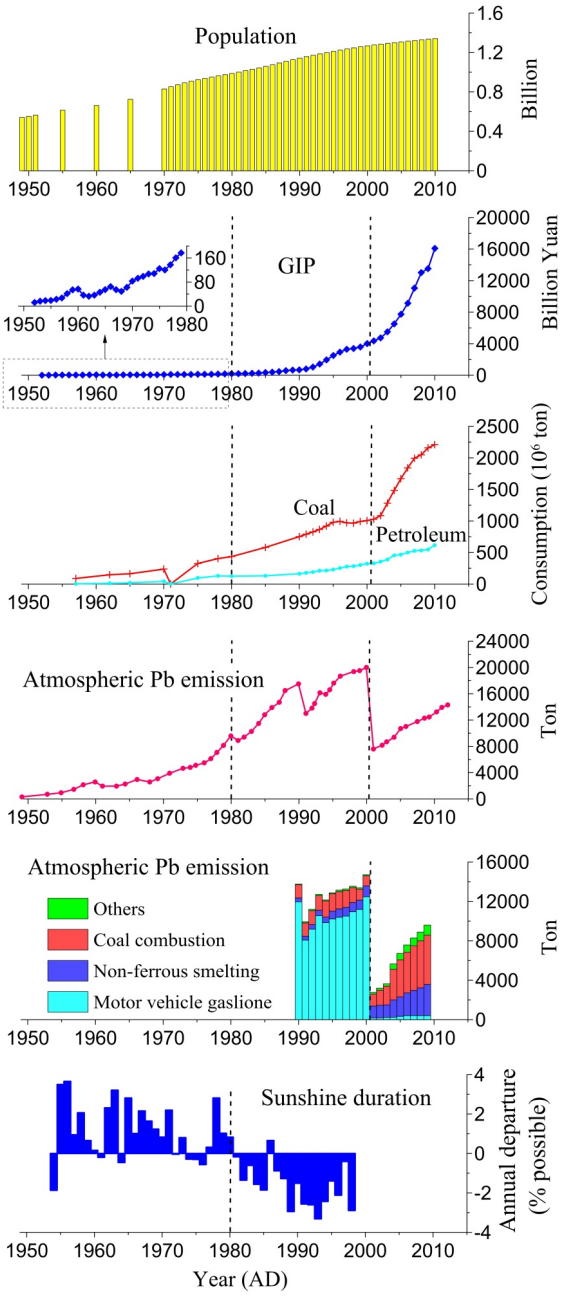
Population
Billion
GIP
Billion Yuan
Coal
Petroleum
Consumption (10^6 ton)
Atmospheric Pb emission
Ton
Atmospheric Pb emission
Others
Coal combustion
Non-ferrous smelting
Motor vehicle gaslione
Ton
Sunshine duration
Annual departure (% possible)
Year (AD)

470

Fig. 5 Population, gross industrial product (GIP), coal and petroleum consumption (standard coal) in China (National Bureau of Statistics China, 2005), estimated atmospheric Pb emissions in China (Tian et al., 2015), estimated atmospheric Pb emissions from different sources in China (Li et al., 2012), and annual departures in percent of sunshine duration in 1954-1998 over the whole China (Kaiser and Qian, 2002).

In the 1950s, anthropogenic Pb fluxes in all the six regions increased obviously compared to that pre-1950, but in the following two decades they remained the same or only experienced slight increases/decreases in the late 1970s except in the Qinghai-Tibet Plateau (Fig. 2 and 4). These changes indicate that the atmospheric Pb pollution in China started to become ubiquitous since the 1950s. This change fitted well with the first rapid development period (1949-1958) of society and economy, especially heavy industry, after the foundation of the People's Republic of China. However, in the following years of 1959-1976 the economy almost stopped developing due to the Great Chinese Famine (1959–1961) and the Chinese Cultural Revolution (1966–1976) (Fig. 5 and 6), resulting in no further deterioration inf atmospheric Pb pollution in the 1960s and 1970s in the regions except for the Qinghai-Tibet Plateau.

Deleted: the

Deleted: o

Deleted: ing

Deleted: in

Deleted: o

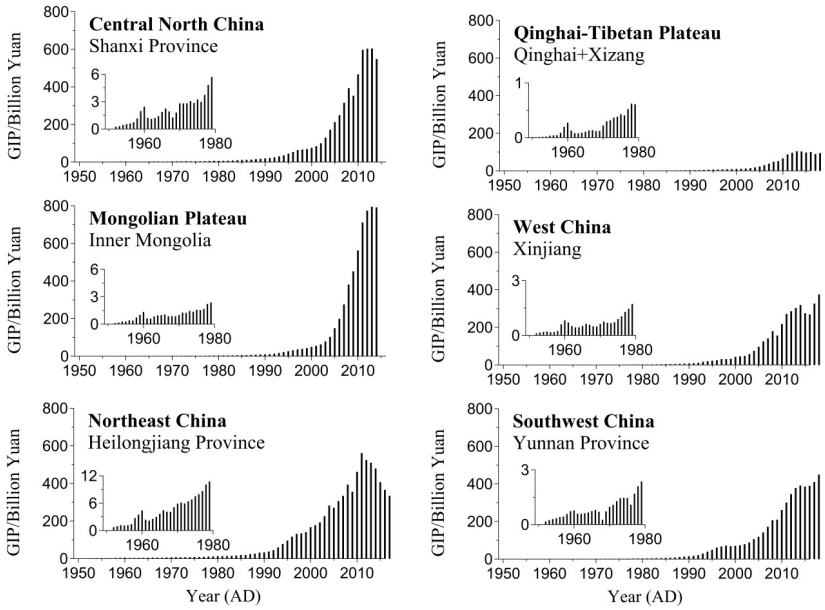

494

495 **Fig. 6** Gross industrial product (GIP) of typical provinces from the six regions of China

496 (National Bureau of Statistics China, 2005).

497

498 In the Qinghai-Tibet Plateau, the anthropogenic Pb fluxes increased in the 1960s

499 and 1970s (Fig. 2 and 4), although its GIP (Qinghai and Xizang) was the lowest and

500 showed similar trend as that in other regions (Fig. 6). Similarly, the ice core of PR in

501 the Central Qinghai-Tibet Plateau also recorded a similar increase trend of

502 anthropogenic Pb during the 1960s-1970s that indicates Pb EF increases of 28% in the

503 1960s and 48% in the 1970s compared to that in the 1950s (Beaudon et al., 2017).

504 Previous studies suggest that this Pb increase may be related to metallurgical activities

505 in Former Soviet Union (e.g., Kyrgyzstan, Tajikistan, Uzbekistan, and Turkmenistan),

506 industrial emission increases in East, South and Southwest Asia, and local activities on

Deleted: +

Deleted: ing

Deleted: inferred

the plateau, derived from back trajectory analysis (Beaudon et al., 2017; Jin et al., 2010; Zhang et al., 2014). Our comparison with the Pb evolution trends in other regions of China, combined with the atmospheric circulation (Fig. 1), further indicates that the Pb increase in the 1960s and 1970s on the plateau was more likely caused by increased atmospheric Pb transport from overseas such as southwest Asia.

In ~1980-2000, anthropogenic Pb fluxes experienced similar accelerated increases in all the six regions of China (Fig. 4). Compared with the 1950s-1970s, Pb fluxes in ~1980-2000 increased by 65% in Northeast China, 208% in West China, 136% on the Mongolian Plateau, 195% on the Qinghai-Tibet Plateau, 310% in central North China and 180% in Southwest China, respectively. Compared with the other stages over the last century, the increase magnitude of the fluxes during this period was the greatest, and the $^{206}Pb/^{207}Pb$ ratios also experienced the most obvious decreases in all the records. These changes imply the rapidest intensification of atmospheric Pb pollution in inland China.

With the implementation of the Reform and Opening-up policy in 1978, China began to enter a rapid industrialization and urbanization period with an average annual growth rate of China's economy of nearly 10%, ranking number one in the world (Fig. 5) (WGEDHC, 2007). Owing to lack of advanced technologies and equipment and taking no account of environmental protection, the development depended mainly on extensive economic growth characterized by high energy consumption, cost and pollution, but low economic efficiency (WGEDHC, 2007). For example, even in 2006 China emitted 6-33 times the amount of air pollutants per unit of GDP as the United

Deleted: combined with

Deleted: ing

Deleted: the

Deleted: the

Deleted: ing

States (Lin et al., 2014). Hence, the rapid socioeconomic development resulted in a great increase in emissions of Pb and other pollutants. In 2000, emissions of industrial dust and atmospheric Pb reached 10.92 million tons and ~20000 tons, respectively (National Bureau of Statistics China, 2003; Tian et al., 2015), ranking number one in the world. Significant decreases in sunshine duration, defined as the amount of time the disk of the sun is above the horizon and not obscured by naturally occurred obstructions such as clouds, fog, and haze, one of the oldest types of radiation measurements, were observed from over 200 meteorological stations over the whole China after ~1980 compared to those pre-1980 (Fig. 5), and those were likely an evidence for the worsening of air pollution related to increased anthropogenic atmospheric pollutants in China (Kaiser and Qian, 2002). Although the decreased sunshine duration may be mainly affected by urban atmospheric pollution, it still has a meaning to that in remote areas of China as Pb pollution in remote records are mainly derived from urban human activities via atmospheric transport.

After ~2000, the anthropogenic Pb fluxes generally stopped increase in all the six regions of China and even decreased slightly in Southwest and Northeast China and the Qinghai-Tibet Plateau, and the $^{206}Pb/^{207}Pb$ ratios was also similar to that in the 1990s except in EH (Fig. 2 and 4). These variations indicate that atmospheric Pb pollution in inland China stopped worsening, even though the economy developed more rapidly than pre-2000 (Fig. 5). Although the QH cores were sampled in 2003, the top 0-0.5 cm sediment sample was formed after 2002 according to the dating result. This change was resulted from the phasing out of leaded gasoline in 2000, which led to a sharp decrease

Deleted: ring

Deleted: is

Deleted: ing

Deleted: ing

in anthropogenic Pb emissions. Li et al. (2012) and Tian et al. (2015) estimated that atmospheric emissions of anthropogenic Pb in China decreased by more than 50% in 2001 compared to those in 2000 (Fig. 5).

The coherent changes of atmospheric Pb pollution after ~2000 in different regions (Fig. 2 and 4) reflect the effectiveness of the phasing out of leaded gasoline in China. However, unlike the change of Pb emissions from gasoline sources, atmospheric Pb did not show a similar sharp decrease after ~2000, but remained at a high level, and even increased again in recent years in some high-resolution records such as GH and SR (Fig. 2). Similarly, an investigation of Pb variations in aerosol samples in the city of Tianjin between 1994 and 2001 also shows no obvious decrease in Pb concentrations after the phasing out of leaded gasoline in 1998 (Wang et al., 2006). This difference is probably caused by (1) resuspension of legacy Pb in ground-surface environments and (2) increase anthropogenic Pb emissions from other sources, such as industry and coal burning in recent years (Fig. 5) (Li et al., 2015; Tian et al., 2015).

Deleted: on controlling atmospheric Pb pollution

Deleted: instead

Deleted: ing

4.3. Spatial variations of atmospheric Pb pollution over China

Besides the differences in the temporal evolution trends among the six regions discussed above, another notable difference in the atmospheric Pb pollution is the differences in Pb increase levels among these regions over the last century. According to the statistical Pb fluxes in Fig 4, it can be seen that the lowest increase in atmospheric Pb was found in the southeast Mongolia Plateau (DL, 2.4 mg m^{-2} yr^{-1} in the 21st Century) and in West China (SR, ~3.4 mg m^{-2} yr^{-1} in the 21st Century) (Zeng et al., 2014) (Table

Deleted: between these regions

Deleted: should be

Deleted: t

Deleted: magnitudes of

591 1), implying the lowest atmospheric Pb levels in these regions. These low values were
592 related to the fact that these areas are relatively far from and upwind of major industrial
593 zones, corresponding to low air pollution levels in these regions as indicated by the
594 spatial variations of $PM_{2.5}$ in Fig. 1 (Ma et al., 2016).

595 **Table 1** Anthropogenic Pb fluxes in the 21st Century in lake sediment records from
596 different regions of China

Region	**Sediment core**	**Anthropogenic Pb flux (**mg m^{-2} yr^{-1}**)**	**Data source**
Central North China	GH	10.2±0.8	This study
	MY	14.2±1.8	This study
	Average	12.1±2.5	
Southeast Mongolian Plateau	DL	2.4±0.1	This study
Northeast China	WDLC-3	7.0±2.2	This study
	WDLC-5	6.4±0.9	This study
	Average	6.7±1.6	
Qinghai -Tibet Plateau	QH03-02	9.8*	Jin et al., 2010
	QH03-14	8.6*	Jin et al., 2010
	NR	20.9±1.5	Zhang et al., 2014
	CHZ	14.1±3.3	Bing et al., 2016
	Average	14.4±3.8	
West China	SR	3.4±0.7	Zeng et al., 2014
Southwest China	EH	16.6±3.8	Li et al., 2017
	FX	26.4±3.2	Liu et al., 2013
	QS	53.2±10.5	Liu et al., 2013
	Average	36.5±19.0	

597 * These values were recalibrated by subtracting average fluxes during ~1750-
598 ~1950 in QH03-02 and during ~1900-~1950 in QH03-14, respectively.

The medium increase of anthropogenic Pb flux was found in Northeast China (6.7±1.6 mg m^{-2} yr^{-1} in the 21st Century), central North China (12.1±2.5 mg m^{-2} yr^{-1} in the 21st Century) and the Qinghai-Tibetan Plateau (14.4±3.8 mg m^{-2} yr^{-1} in the 21st Century), which were several times higher than those in the above two regions, suggesting a higher level of atmospheric Pb. It is reasonable that the atmospheric Pb level is high in the Northeast and central North China, as (1) ~1/4 of China's coal is produced in central North China (Shanxi Province) and a large amount of coal is also consumed here and (2) Northeast China is an important base of heavy industry and steel production accounting for more than a quarter of the country. An exception is the Qinghai-Tibetan Plateau. Although it is one of most underdeveloped regions in China, the 21st-Century anthropogenic Pb fluxes are as high as ~10-20 mg m^{-2} yr^{-1} recorded by QH, NR, and CHZ (Table 1) (Bing et al., 2016; Zhang et al., 2014). The high anthropogenic Pb fluxes in the region are likely related to the following reasons: (1) many atmospheric pollutants are transported from both East China by the east Asian monsoon and southwest Asian countries by the southwest India monsoon (Beaudon et al., 2017; Yang et al., 2010) and (2) the plateau is an atmospheric deposition area, as indicated by widely distributed loess deposits and modern eolian dust monitoring (Stauch, 2015; Wan et al., 2012).

The greatest increase of Pb flux was found in Yunnan Province in Southwest China. The anthropogenic Pb fluxes in the 21st Century were 26.4 mg m^{-2} yr^{-1} in FX, 53.2 mg m^{-2} yr^{-1} in QS and 16.6 mg m^{-2} yr^{-1} in EH (Li et al., 2017; Liu et al., 2013), with

Deleted: every year

Deleted: in this area

Deleted: s

an average of 36.5±19.0 mg m^{-2} yr^{-1}, implying a very high level of current atmospheric Pb in this region. Yunnan Province is one of the three most important bases of nonferrous industry and described as the nonferrous kingdom in China. In 2013, the output of the major ten nonferrous metals was 3.2 million tons in this province, accounting for 7.25% of the country and ranking the third in China (YBQTS, 2015). The large amounts of ore mining and smelting activities were an important cause of the severe atmospheric Pb pollution in this region (Li et al., 2017; Liu et al., 2013). This suggests that potentially toxic trace metals emitted by mining and metallurgical industry in this region should be given special attention in the future environmental management.

It should be noted that the above spatial distribution results are preliminary, owing to (1) relatively sparse records and (2) the fact that the reconstructed fluxes may be affected by the remoteness of the lakes. In the future, more high-resolution reconstructions and direct observations in remote areas, especially on the Qinghai-Tibetan Plateau, are needed to obtain a more accurate spatial picture of atmospheric Pb pollution in China.

4. Conclusions

This study revealed temporal and spatial variations of atmospheric Pb pollution in China during the last century based on Pb data from 17 sediment records from relatively remote areas in inland China. Although Pb concentrations varied substantially among different records, the sediment profiles of Pb EFs, anthropogenic fluxes, and isotopic

Deleted: C

Deleted: ary

compositions in these records except that in the Qinghai-Tibet Plateau show similar evolution trends over the last century, implying a synchronous atmospheric Pb evolution in most areas of China. These records suggest that the atmospheric Pb pollution occurred occasionally before 1950. The widespread pollution in China began in the 1950s, corresponding to the beginning development of society and economy after the foundation of New China in 1949. However, rapid increases of the atmospheric Pb occurred after the 1980s, owing to quick development of extensive economy after the Reform and Opening-up in 1978. After 2000, the atmospheric Pb generally stopped increase due to the phasing out of leaded gasoline, but it remained high and even likely started to increase again in recent years. Assessment of spatial variations of the atmospheric Pb over China suggests the lowest level in the southeast Mongolia Plateau and in West China, a medium level in Northeast China and central North China, and the highest level in Southwest China.

Deleted: C

Deleted: inland

Deleted: only

Deleted: did not

Deleted: until

Deleted: ing

Deleted: o

Acknowledgements

This work was financially supported by Basic Research Program of Institute of Hydrogeology and Environmental Geology CAGS [SK201503], National Natural Science Foundation of China [41405123], and Project from the Ministry of Ecology and Environment [DQGG0104]. We thank Dr. Fei Zhang at Institute of Earth Environment CAS and Mr. Guanglin Yang at 101 Geological Team of Sichuan Province Bureau of Geology and Mineral Resources for their assistance in laboratory analysis

675 and field sampling. We thank Yang Liu and Zongwei Ma who kindly provided us with
676 the $PM_{2.5}$ level map of China.

677 **Declarations of interest: None**

678 **References**

679 Anjum, R., Gao, J., Tang, Q., He, X., Zhang, X., Long, Y., et al., 2017. Linking
680 sedimentary total organic carbon to 210Pbex chronology from Changshou Lake in
681 the Three Gorges Reservoir Region, China. Chemosphere, 174, 243-252.
682 Appleby, P.G., 2001. Chronostratigraphic techniques in recent sediments-Tracking
683 environmental change using lake sediments. Springer, Netherlands, 171-203.
684 Bao, K., Shen, J., Wang, G., Le Roux, G., 2015.Atmospheric deposition history of trace
685 metals and metalloids for the last 200 years recorded by three peat cores in Great
686 Hinggan Mountain, Northeast China. Atmosphere 6, 380–409.
687 Bao, K., Shen, J., Wang, G., Tserenpil, S. (2016). Anthropogenic, detritic and
688 atmospheric soil-derived sources of lead in an alpine poor fen in northeast China.
689 Journal of Mountain Science, 13(2), 255-264.
690 Beaudon, E., Gabrielli, P., Sierra-Hernández, M. R., Wegner, A., Thompson, L. G.
691 (2017). Central Tibetan Plateau atmospheric trace metals contamination: a 500-year
692 record from the Puruogangri ice core. Science of the Total Environment, 601, 1349-
693 1363.

694 Bing, H., Wu, Y., Zhou, J., Li, R., & Wang, J., 2016. Historical trends of anthropogenic
695 metals in Eastern Tibetan Plateau as reconstructed from alpine lake sediments over
696 the last century. Chemosphere, 148, 211-219.
697 Chen, J., Tan, M., Li, Y., Zhang, Y., Lu, W., Tong, Y., et al., 2005. A lead isotope record
698 of Shanghai atmospheric lead emissions in total suspended particles during the
699 period of phasing out of leaded gasoline. Atmospheric Environment, 39(7), 1245-
700 1253.
701 Chen, M., Boyle, E. A., Switzer, A. D., Gouramanis, C., 2016. A century long
702 sedimentary record of anthropogenic lead (Pb), Pb isotopes and other trace metals in
703 Singapore. Environmental Pollution, 213, 446-459.
704 Chen L, Zhu Q, Luo H, et al., 1991. East Asian monsoon. Beijing: China Meteorological
705 Press.
706 Cheng, H., Hu, Y. (2010). Lead (Pb) isotopic fingerprinting and its applications in lead
707 pollution studies in China: a review. Environmental Pollution, 158(5), 1134-1146.
708 Ferrat, M., Weiss, D.J., Dong, S., Large, D.J., Spiro, B., Sun, Y., Gallagher, K., 2012.
709 Lead atmospheric deposition rates and isotopic trends in Asian dust during the last
710 9.5 kyr recorded in an ombrotrophic peat bog on the eastern Qinghai-Tibetan Plateau.
711 Geochimica et Cosmochimica Acta 82, 4–22.
712 García-Alix, A., Jiménez-Espejo, F. J., Lozano, J. A., Jiménez-Moreno, G., Martínez-
713 Ruiz, F., Sanjuán, L. G., et al. (2013). Anthropogenic impact and lead pollution
714 throughout the Holocene in Southern Iberia. Science of the total environment, 449,
715 451-460.

716 Gui, Z., Xue, B., Yao, S., Zhang, F., Yi, S. (2012). Catchment erosion and trophic status
717 changes over the past century as recorded in sediments from Wudalianchi Lake, the
718 northernmost volcanic lake in China. Quaternary International, 282, 163-170.
719 Hillman, A. L., Abbott, M. B., Yu, J., Bain, D. J., Chiou-Peng, T., 2015. Environmental
720 legacy of copper metallurgy and Mongol silver smelting recorded in Yunnan lake
721 sediments. Environmental science & technology, 49(6), 3349-3357.
722 Jin, Z., Han, Y., Chen, L. (2010). Past atmospheric Pb deposition in Lake Qinghai,
723 northeastern Tibetan plateau. Journal of Paleolimnology, 43(3), 551-563.
724 Kaiser, D. P., Qian, Y. (2002). Decreasing trends in sunshine duration over China for
725 1954–1998: Indication of increased haze pollution?. Geophysical Research Letters,
726 29(21), 38-1–38-4, doi:10.1029/2002GL016057.
727 Lan, B., Zhang, D., Yang, Y., 2018. Lacustrine sediment chronology defined by 137Cs,
728 210Pb and 14C and the hydrological evolution of Lake Ailike during 1901–2013,
729 northern Xinjiang, China. Catena, 161, 104-112.
730 Lee, C.L., Qi, S.H., Zhang, G., Luo, C.L., Zhao, L.L., Li, X.D., 2008. Seven thousand
731 years of records on the mining and utilization of metals from lake sediments in
732 central China. Environmental Science and Technology 42, 4732-4738.
733 Li, K., Liu, E., Zhang, E., Li, Y., Shen, J., Liu, X. (2017). Historical variations of
734 atmospheric trace metal pollution in Southwest China: reconstruction from a 150-
735 year lacustrine sediment record in the Erhai Lake. Journal of Geochemical
736 Exploration, 172, 62-70.

737 Li, Q., Cheng, H., Zhou, T., Lin, C., Guo, S., 2012. The estimated atmospheric lead
738 emissions in China, 1990–2009. Atmospheric Environment 60, 1-8.
739 Li, Y., Zhou, S., Zhu, Q., Li, B., Wang, J., Wang, C., Chen L., Wu, S. (2018). One-
740 century sedimentary record of heavy metal pollution in western Taihu Lake, China.
741 Environmental Pollution, 240, 709-716.
742 Lin, J., Pan, D., Davis, S. J., Zhang, Q., He, K., Wang, C., et al. (2014). China's
743 international trade and air pollution in the United States. Proceedings of the National
744 Academy of Sciences, 111(5), 1736-1741.
745 Liu, E., Zhang, E., Li, K., Nath, B., Li, Y., Shen, J. (2013). Historical reconstruction of
746 atmospheric lead pollution in central Yunnan province, southwest China: an analysis
747 based on lacustrine sedimentary records. Environmental Science and Pollution
748 Research, 20(12), 8739-8750.
749 Liu X, Dong S, Guo D, Li B, Adams F., 2004. Characterization of pollution episode
750 with combined lead and biomass burning contributions based on chemical and
751 isotopic data. J Chinese Mass Spectrom Soc 23(1): 6-11 (in Chinese with English
752 abstract).
753 Lv Y, Kong T, Rang W, 2013. Analysis of the epidemic characteristics of blood lead
754 excess in China from 2004 to 2012. Chin Prev Med, 14(11), 868-870 (in Chinese).
755 Ma Z, Hu X, Sayer AM, Levy R, Zhang Q, Xue Y, Tong S, Bi J, Huang L, Liu Y. 2016.
756 Satellite-based spatiotemporal trends in $PM_{2.5}$ concentrations: China, 2004–2013.
757 Environ Health Perspect 124, 184–192, http://dx.doi.org/10.1289/ehp.1409481.

758 Marx, S. K., Rashid, S., Stromsoe, N. (2016). Global-scale patterns in anthropogenic
759 Pb contamination reconstructed from natural archives. Environmental pollution, 213,
760 283-298.
761 McConnell, J. R., Wilson, A. I., Stohl, A., Arienzo, M. M., Chellman, N. J., Eckhardt,
762 S., et al. (2018). Lead pollution recorded in Greenland ice indicates European
763 emissions tracked plagues, wars, and imperial expansion during antiquity.
764 Proceedings of the National Academy of Sciences, 115(22), 5726-5731.
765 Mukai, H., Tanaka, A., Fujii, T., Zeng, Y., Hong, Y., Tang, J., et al., 2001. Regional
766 characteristics of sulfur and lead isotope ratios in the atmosphere at several Chinese
767 urban sites. Environmental Science & Technology, 35(6), 1064-1071.
768 National Bureau of Statistics China, 2003. Environmental statistics (2003).
769 http://www.stats.gov.cn/ztjc/ztsj/hjtjzl/2003/200507/t20050706_53168.html.
770 National Bureau of Statistics China, 2005. Environmental statistics (2005).
771 http://www.stats.gov.cn/ztjc/ztsj/hjtjzl/2005/.
772 Pérez-Rodríguez, M., Silva-Sánchez, N., Kylander, M. E., Bindler, R., Mighall, T. M.,
773 Schofield, J. E., et al. (2018). Industrial-era lead and mercury contamination in
774 southern Greenland implicates North American sources. Science of the Total
775 Environment, 613, 919-930.
776 Pompeani, D. P., Abbott, M. B., Steinman, B. A., Bain, D. J. (2013). Lake sediments
777 record prehistoric lead pollution related to early copper production in North America.
778 Environmental Science & Technology, 47(11), 5545-5552.

779 Pratte, S., Bao, K., Shen, J., Mackenzie, L., Klamt, A. M., Wang, G., Xing, W. (2018).
780 Recent atmospheric metal deposition in peatlands of northeast China: A review.
781 Science of The Total Environment, 626, 1284-1294.
782 Rauch, J.N., Pacyna, J.M. (2009). Earth's global Ag, Al, Cr, Cu, Fe, Ni, Pb, and Zn
783 cycles. Global Biogeochemical Cycles, 23(2), GB2001.
784 Sierra-Hernández, M.R., Gabrielli, P., Beaudon, E., Wegner, A., Thompson, L. G.
785 (2018). Atmospheric depositions of natural and anthropogenic trace elements on the
786 Guliya ice cap (northwestern Tibetan Plateau) during the last 340 years. Atmospheric
787 Environment, 176, 91-102.
788 Stauch, G. (2015). Geomorphological and palaeoclimate dynamics recorded by the
789 formation of aeolian archives on the Tibetan Plateau. Earth-Science Reviews, 150,
790 393-408.
791 Tian, H., Zhu, C., Gao, J., Cheng, K., Hao, J., Wang, K., et al. (2015). Quantitative
792 assessment of atmospheric emissions of toxic heavy metals from anthropogenic
793 sources in China: historical trend, spatial distribution, uncertainties, and control
794 policies. Atmospheric Chemistry and Physics, 15(17), 10127-10147.
795 Wan, D., Jin, Z., Wang, Y. (2012). Geochemistry of eolian dust and its elemental
796 contribution to Lake Qinghai sediment. Applied geochemistry, 27(8), 1546-1555.
797 Wan D, Han Z, Yang J, Yang G, Liu X, 2016a. Heavy metal pollution in settled dust
798 associated with different urban functional areas in a heavily air-polluted city in North
799 China. International Journal of Environmental Research and Public Health, 13(11),
800 1119, doi:10.3390/ijerph13111119.

Wan D, Jin Z, Zhang F, Song L, Yang J, 2016b. Increasing dust fluxes on the northeastern Tibetan Plateau linked with the Little Ice Age and recent human activity since the 1950s. Aeolian Research, 23, 93–102.

Wan D, Song L, Yang J, Jin Z, Zhan C, Mao X, Liu D, Shao Y, 2016c. Increasing heavy metals in the background atmosphere of central North China since the 1980s: evidence from a 200-year lake sediment record. Atmospheric Environment, 138, 183–190.

Wan D, Mao X, Jin Z, Song L, Yang J, Yang H, 2019a. Sedimentary biogeochemical record in Lake Gonghai: implications for recent lake changes in relatively remote areas of China. Science of the Total Environment, 649, 929-937.

Wan D, Song L, Mao X, Yang J, Jin Z, Yang H, 2019b. One-century sediment records of heavy metal pollution on the southeast Mongolian Plateau: implications for air pollution trend in China, Chemosphere, 220, 539-545.

Wang,W., Liu, X., Lu, Y., Guo, D., Li, Y., Tian, X., Adans, F., 2002. Determination of lead isotope abundance ratio of atmospheric aerosol and lead source study. Zhi Pu Xue Bao 23, 21–29 (in Chinese with English abstract).

Wang, W., Liu, X., Zhao, L., Guo, D., Tian, X., Adams, F., 2006. Effectiveness of leaded petrol phase-out in Tianjin, China based on the aerosol lead concentration and isotope abundance ratio. Science of the Total Environment, 364(1-3), 175-187.

Weiss, D., Shotyk, W., Kempf, O. (1999). Archives of atmospheric lead pollution. The Science of Nature, 6(86), 262-275.

WGEDHC (Writing Group of Economic Development History of China), 2007. Economic development history of China (1949-2005). Shanghai: Shanghai University of Finance and Economics Press.

WGEDHC (Writing Group of Economic Development History of China), 2016. Economic development history of China (1840-1949). Shanghai: Shanghai University of Finance and Economics Press.

Yang, H., Battarbee, R. W., Turner, S. D., Rose, N. L., Derwent, R. G., Wu, G., Yang, R. (2010). Historical reconstruction of mercury pollution across the Tibetan Plateau using lake sediments. Environmental Science & Technology, 44(8), 2918-2924.

Yao, S., Xue, B. (2014). Heavy metal records in the sediments of Nanyihu Lake, China: influencing factors and source identification. Journal of Paleolimnology, 51(1), 15-27.

Yu, R., Hu, G., Yang, Q., He, H., Lin, C., 2016. Identification of Pb sources using Pb isotopic compositions in the core sediments from Western Xiamen Bay, China. Marine pollution bulletin, 113(1-2), 247-252.

Yunnan Bureau of Quality and Technical Supervision (YBQTS), 2015. Quality analysis report of nonferrous metallurgy industry in Yunnan Province.

Zeng, H., Wu, J., Liu, W. (2014). Two-century sedimentary record of heavy metal pollution from Lake Sayram: A deep mountain lake in central Tianshan, China. Quaternary International, 321, 125-131.

Zheng, J., Tan, M., Shibata, Y., Tanaka, A., Li, Y., Zhang, G., Zhang, Y., Shan, Z., 2004. Characteristics of lead isotope ratios and elemental concentrations in PM_{10} fraction

of airborne particulate matter in Shanghai after the phase-out of leaded gasoline. Atmospheric Environment 38, 1191–1200.

Zhang, H., Shan, B., Ao, L., Tang, W., Wen, S. (2014). Past atmospheric trace metal deposition in a remote lake (Lake Ngoring) at the headwater areas of Yellow River, Tibetan Plateau. Environmental Earth Sciences, 72(2), 399-406.

Zhang, R., Guan, M., Shu, Y., Shen, L., Chen, X., Zhang, F., et al., 2016. Reconstruction of historical lead contamination and sources in Lake Hailing, Eastern China: a Pb isotope study. Environmental Science and Pollution Research, 23(9), 9183-9191.